Prepared for ASME Annual
Natl. Symp., College Park, Md.

N80

HYDROGEN CONVECTIVE COOLING OF ROCKET NOZZLES

By W. A. Benser and R. W. Graham

Lewis Research Center
National Aeronautics and Space Administration
Cleveland, Ohio

ABSTRACT

Space propulsion requirements have placed a great deal of emphasis on hydrogen as a fuel because of its high impulse in both chemical and nuclear rocket systems. Hydrogen is also attractive as a coolant because it has a high heat capacity and a high thermal conductivity. In systems which use hydrogen as a propellant, convective cooling with hydrogen is the most desirable nozzle cooling system.

The design of a convectively cooled rocket nozzle is based on calculation of a balance between the heat flux from the hot gas to the nozzle wall and the heat flux from the wall to the coolant. To perform these heat balance calculations, accurate estimates of the heat transfer coefficients for both the hot gas and the coolant are necessary. An accurate estimate of the coolant pressure drop is also essential.

In this paper, methods of predicting the hot gas side heat transfer coefficients are evaluated in terms of experimental data. Heat transfer and pressure loss correlations developed from heated tube experiments with hydrogen as a coolant are also presented. The application of these techniques to a nozzle design is considered, and the shortcomings of the design method are discussed.

INTRODUCTION

Hydrogen is an extremely attractive propellant for both nuclear and chemical space propulsion systems because it produces a very high

specific impulse. Hydrogen also has an extremely large heat sink capacity and high thermal conductivity which makes it an attractive coolant. In the design of the nozzle cooling system for a propulsion system that uses hydrogen as a propellant, it is logical to utilize convective cooling with hydrogen as the coolant. The objective of this paper is to review the state of the art in regards to the design of such a nozzle cooling system.

The design process consists of specifying a wall temperature distribution and computing the coolant channel geometry so that a balance exists between the heat flux into the nozzle wall and the heat flux carried away by the coolant. For convenience of calculation of these heat balances, the heat flux on both the hot gas and coolant sides of the wall are usually expressed in terms of heat transfer coefficients. The conduction across the nozzle wall, and the pressure drop along the coolant channel must also be accurately estimated.

Two methods of predicting hot gas side heat transfer coefficients are considered. The simplest is based on a turbulent flow Nusselt number type of correlation and the second is based on approximate solutions of the boundary layer energy and momentum equations. Experimental data are compared with the values predicted by both methods.

Evaluation of the coolant side heat transfer coefficient is complicated by the fact that the thermodynamic state of the hydrogen will most likely be close to the critical temperature. In this region the thermodynamic and transport properties of the fluid vary abruptly with temperature and pressure. Extrapolation of the standard convective heat transfer correlations therefore, is very unreliable. Studies of heat transfer

to hydrogen have been made for a wide range of conditions (refs. 1, 2, 3, 4, and 5). These results are summarized and problems of application to designs are discussed.

The correlations considered most applicable at the present time are applied to a sample calculation, and the shortcomings of the available techniques are discussed.

The calculations and comparisons presented herein were made by members of the Rocket Heat Transfer Branch of the Lewis Research Center.

SYMBOLS

A	flow area
a, b, c	arbitrary exponents
C	coefficient
c_p	specific heat at constant pressure
d	diameter
h	heat transfer coefficient based on temperature difference
h_i	heat transfer coefficient based on enthalpy difference
i	enthalpy
k	thermal conductivity
l	length
m	molecular weight
Nu	Nusselt number, $\frac{hd}{k}$
Nu_i	Nusselt number based on enthalpy, $\frac{h_i c_p d}{k}$
P	pressure
Pr	Prandtl number, $\frac{c_p \mu}{k}$
q	local heat flux

Re	Reynolds number, $\frac{\rho V d}{\mu}$
r	radius
T	temperature
V	velocity
$\dot{w}$	weight flow rate
x	quality of two phase fluid (mass fraction)
x_2	pseudo quality
μ	absolute viscosity
ρ	density
ρ_{fm}	corrected density (boiling)
X_{tt}	Martinelli two phase parameter, both phases turbulent

Subscripts:

ad	adiabatic wall condition
av	average
BL	boundary layer
b	bulk
calc	calculated
ex	experimental
f	film
g	gas
i, ref	reference enthalpy condition
l	liquid
melt	melting point condition
N-1D	Nusselt correlation one-dimensional
N-3D	Nusselt correlation three-dimensional
o	stagnation condition

pg perfect gas

ref reference condition

s static or stream condition

t throat

w wall condition

Superscript:

' supercritical pseudo two-phase

DISCUSSION

As was specified in the INTRODUCTION, the design procedure for a regeneratively cooled rocket nozzle first involves specifying a wall temperature. Next the heat transfer coefficient on the gas-side is estimated. This enables the designer to estimate the heat flux from the gas to the wall. An iterative procedure follows such that the coolant-side heat transfer coefficient is determined to set the wall temperature at the desired level. This procedure is repeated at local stations throughout the nozzle. For discussion purposes, methods for estimating the gas-side and liquid-side heat transfer coefficients will be discussed separately.

Hot Gas-Side Heat Transfer

The heat flux can either be computed from some established heat transfer coefficient correlation such as the conventional Nusselt number correlations for turbulent flow, or it can be calculated from an approximate solution of the boundary layer energy and momentum equations. For most heat transfer calculations the driving potential is based on the difference between gas and wall temperature. The propellant gas in rocket nozzles may be partially dissociated, and chemical reactions in

the boundary layer may contribute appreciably to the heat flux to the wall. Eckert and Drake (ref. 6) stated that for heat flux from reacting gases, the enthalpy difference should be used rather than the temperature difference. This has been confirmed by Brokaw (ref. 7). The use of driving enthalpy produces no particular difficulties for nonreacting gases. Inasmuch as the use of driving enthalpy is equally applicable to nonreacting gases and to reacting gases, enthalpy difference will be used as the driving potential in this discussion.

Turbulent flow heat transfer correlations. - When enthalpy is used as the driving potential, local heat flux can be expressed as

$$q = h_i(i_{ad} - i_w) \tag{1}$$

For a turbulent boundary layer, the heat transfer coefficient h_i is expressed in terms of flow conditions, geometry, and gas properties by the equation

$$Nu_i = C\ Re^{0.8}Pr^{0.333} \tag{2}$$

The value of the coefficient C in this equation and the reference dimension in the Reynolds and Nusselt numbers are dependent on the flow system under consideration. For fully developed flow in a constant diameter pipe (i.e., where the boundary layer thickness is equal to the pipe radius and there are no appreciable axial pressure gradients), C is considered to be a constant and the reference dimension is taken as the pipe diameter. The conditions of fully developed flow and constant area do not apply for a convergent divergent rocket nozzle. However, most nozzle heat transfer calculations have been based on the assumption that C is constant throughout the nozzle and local nozzle diameter is used as the reference dimension.

Available heat transfer data for rocket nozzles indicate a range of values for C. Bartz (ref. 8) gives a value of 0.026 for a particular family of nozzles. His value is based on boundary layer analysis. Inasmuch as the exact value of C and the variation of this coefficient with nozzle geometry and axial position is not well established at this time, a value of 0.026 will be used in this discussion. Furthermore, the local nozzle diameter will be used as the reference dimension, and gas transport properties will all be based on a reference condition. Therefore

$$Nu_i = \frac{h_i c_{p,ref} d}{k_{ref}} \tag{3}$$

By use of the perfect gas law and equations 2 and 3

$$h_i = \frac{0.026(\rho_s V_s)^{0.8}(\mu)^{0.2}_{ref}}{d^{0.2} Pr^{0.667}_{ref}} \left(\frac{\frac{T_s}{m_s}}{\frac{T_{ref}}{m_{ref}}} \right)^{0.8} \tag{4}$$

Reference 6 (pp. 261-272) recommends that transport properties be evaluated at a reference enthalpy given by

$$i_{ref} = i_s + 0.5(i_w - i_s) + 0.22\ Pr^{1/3}_{i,ref}(i_o - i_s) \tag{5}$$

therefore, in equation (4), μ, Pr, and (T/m) are evaluated at i_{ref} and static pressure conditions. The value of i_{ad} in equation (1) is evaluated from

$$i_{ad} = i_s + (Pr_{i,ref})^{1/3}(i_o - i_s) \tag{6}$$

There are two possible methods of evaluating the $\rho_s V_s$ term in equation (4). The one-dimensional approach where

$$\rho_s V_s = \frac{\dot{W}}{A} \tag{7}$$

is the simplest and probably most widely used method. The second method is to base $(\rho_s V_s)$ on the axisymmetric or three-dimensional value of ρV at the wall. For conventional convergent-divergent nozzles, the boundary layer at any axial station is very thin compared to the radius of the nozzle. Therefore, $\rho_s V_s$ can either be evaluated from wall pressure measurements and known stagnation conditions, or it can be calculated from flow theory. It should be noted that the values of $\rho_s V_s$ calculated by the one-dimensional or the three-dimensional approaches will not be greatly different in the convergent region of the nozzle where the velocities are subsonic. In the divergent region of conical nozzles the difference will also be relatively small. In the divergent sections of bell nozzle, however, large differences can be obtained as shown in figure 1. This figure shows that the constant $\rho_s V_s$ lines for a conical nozzle are essentially spherical surfaces and, for small divergence angles, do not vary appreciably from the approximation of constant $\rho_s V_s$ along the radius. For the bell nozzle, however, the constant $\rho_s V_s$ lines depart radically from radial lines.

Boundary layer solution of heat flux. - Solution of the boundary layer energy and momentum equations is a more basic approach to evaluation of nozzle heat transfer. Theoretical solutions for laminar boundary layers are fairly well established. However, for nozzle application, the Reynolds numbers are sufficiently large that turbulent boundary

layers will probably prevail. The solution of the momentum and energy equations for the turbulent boundary layers involves several simplifying assumptions. Approximate solutions to the turbulent boundary layer equations are given in references 9, 10, and 11.

The method proposed by Bartz (ref. 11), was developed for rocket nozzle heat transfer calculations and will be used here as representative of the boundary layer approach. This particular method is based on the following assumptions.

1. The gas temperature and the velocity profile follow a 1/7 power law.

2. The local skin friction coefficients are the same as would exist on a flat plate for the same boundary layer thickness.

3. Reynolds analogy between momentum transfer and heat transfer exists for the nozzle boundary layer flow under consideration.

Calculation of heat flux by this method for a particular nozzle requires selection of an initial boundary layer condition and an evaluation of $\rho_s V_s$ at the free stream edge of the boundary layer. Bartz has shown that the initial boundary layer has little effect on the calculated heat flux in the divergent portion of a nozzle. In the convergent region, however, the calculated heat flux is very dependent on the assumed initial boundary layer conditions. Based on the $\rho_s V_s$ variations shown in figure 1, it is recommended that a three-dimensional approach be used to determine the $\rho_s V_s$ values to be used in the calculations.

Comparison with experimental data. - In order to evaluate the applicability of the above techniques of estimating hot gas-side heat

transfer, a comparison with experimental data is necessary. For this discussion, a comparison will be made with data obtained at the Lewis Research Center with a heated air facility. The nozzle tested was a 25 to 1 area ratio bell shaped nozzle designed by the Rao optimum thrust method (ref. 12). Air heated to a maximum total temperature of 1600° R was the working fluid. The nozzle wall was 1/2 inch thick stainless steel and the external surface was cooled by a water bath. Heat transfer through the wall was measured with instrumented Inconel thermal plugs, 1/8 inch diameter, that extended through the nozzle wall and were flush with the inner surface. Each plug has three thermocouples to indicate the thermal gradient. It was possible to insert various upstream geometries near the nozzle entrance to control the flow and boundary layer. Only one upstream geometry will be considered in this discussion. It will be a nuclear reactor flow simulator which has a thick disk drilled with many holes to represent the flow passages in the fuel elements of a nuclear reactor.

Figure 2 shows the experimental heat transfer coefficients distribution throughout the nozzle. The abscissa is expressed as axial distance made dimensionless by dividing by the throat diameter. The positive values of l/d_t are downstream of the throat and the negative values upstream. The peak heat transfer coefficient is somewhat upstream of the geometric throat. This throat distribution is quite similar to that presented by Welsh of J. P. L. in reference 13 for a hydrazine-nitrogen tetraoxide rocket motor.

In figure 3, various ways of estimating the gas-side heat transfer coefficient are compared with the experimental results obtained

with a Rao designed bell nozzle. Included in these methods are simple Nusselt number relations (eq. 2) and the more elaborate boundary layer analysis. Two variations of the simple Nusselt relation are included. In one case the $\rho_s V_s$ product is based upon one-dimensional values and in the other the $\rho_s V_s$ products are three-dimensional values. For the boundary layer analysis, two starting lengths are included to illustrate the sensitivity of the local heat transfer coefficient values (especially upstream of the throat) to this length. In case 1 the boundary layer was assumed to have zero thickness at the downstream face of the core simulator. For case 2, the point of zero boundary layer thickness was assumed to be 10 inches upstream of the exit face of the simulator.

A number of general observations can be made in comparing these various methods of estimating heat transfer coefficients with the experimental results. Table I has been inserted to assist the reader in this comparison.

As shown on figure 3 and in table I the one-dimensional and three-dimensional Nusselt type correlations give the same results up to the nozzle throat (i.e., $l/d_t = 0$). Both underestimate the experimental heat transfer coefficient by about 40 percent at $l/d_t = -1.9$. At the throat the accuracy of the Nusselt correlation is very good. The one-dimensional Nusselt approach overestimates the heat flux for a short distance downstream of the throat. Beyond an l/d_t of 0.5, this approach underestimates the heat transfer coefficient by as much as 50 percent. The three-dimensional Nusselt correlation is good up to a value of l/d_t of 0.5. At higher values of l/d_t, this approach also underestimates the heat flux by as much as 23 percent.

The case 1 boundary layer calculation assumed a zero thickness at the downstream side of the core simulator. This calculation gave a heat transfer coefficient which was 30 percent low at $l/d_t = -1.9$. In the region of the throat and in the divergent portion of the nozzle, this calculation overestimated the heat transfer coefficient by up to 35 percent. The case 2 boundary layer calculation was assumed to have a new thickness 10 inches upstream of the downstream face of the core simulator. This corresponds to an l/d_t of -9.0. For this case the calculated value of heat transfer coefficient was 45 percent low at the $l/d_t = -1.9$ station. From the value of $l/d_t = -0.5$ to the nozzle exit, this calculation gave the best agreement with experiment. The maximum deviation for this region was 16 percent.

These comparisons, figure 3 and Table I, indicate that none of the prediction schemes are sufficiently accurate for the convergent region of the nozzle. For the divergent region of the nozzle the Nusselt number approach based on a three-dimensional evaluation of $\rho_s V_s$ is far superior to that based on a one-dimensional value of $\rho_s V_s$. In the vicinity of the throat and in the divergent region, the best prediction of heat transfer coefficient is obtained by the case 2 boundary layer approach.

Applicability of the Nusselt type correlations can be improved by considering the coefficient C to be a function of axial position in the nozzle. Accurate application of this approach, however, would depend on experimental determination of the correct variation of C for each particular geometry considered. Further modifications to the assumptions used in the boundary layer theory, may also provide better

correlations for the convergent region of the nozzle. Further research on hot gas-side heat transfer is required before reliable prediction of heat flux can be made.

Coolant Side Heat Transfer

It is accepted practice for the rocket designer to estimate heat transfer coefficients for the inside of the coolant passage from correlations derived from heated tube experiments. Obviously, there are a number of similitude criteria that cannot be satisfied in comparing the rocket cooling passages to heated tube test sections. Among the inconsistencies are the differences in geometry and distribution of heat flux, both circumferentially and longitudinally, along the channel. Generally, the heated tube experiment involves nearly uniform heating of the entire test section. More will be said about the limitations of heated tube experimental results to rocket cooling passage design in a later section. Certain limitations not withstanding, the heated tube experiment does provide the most reliable and applicable information currently available for the design of rocket cooling passages.

During the past 3 years, considerable effort has been devoted to the study of hydrogen as a coolant in heated tube experiments. Some of the work is listed in references 1 to 5. In these experiments, hydrogen has been studied as a gas, a liquid, and an above-critical-pressure fluid. In the gaseous regime, the correlations developed from heated tube experiments have been similar to those obtained from other gases including air. Most of the reported correlations were obtained from overall heat transfer results and thus express a heat transfer coefficient that is really an average for the entire test section.

However, for both local and overall heat transfer, the form of the correlations is quite similar and can be expressed in the usual pipe-flow correlation for turbulent flow.

$$Nu = C(Re)^{a}_{ref}(Pr)^{b}_{ref}\left(\frac{l}{d}\right)^{c} \tag{8}$$

The coefficient and exponents for this equation and the fluid state where properties are evaluated, vary from investigator to investigator. Table I of reference 5 gives a partial listing of the correlating equations for gaseous hydrogen. One does have to be careful not to extrapolate any one correlation much beyond the bulk temperature or wall to bulk temperature ratios explored in the actual tests. (Bulk temperature is defined as the integrated average stagnation temperature at any given station.) Serious errors in estimating the heat transfer coefficient could be encountered. This is also discussed in reference 5.

The fact that liquified hydrogen used as a coolant could reach or at least be close to its critical temperature somewhere along the coolant passage does make hydrogen a unique coolant. Attendant to this uniqueness in state are properties and property changes around the critical point that greatly influence the mechanisms of mass and heat transfer and, consequently, make heat transfer predictions difficult. In a real sense, hydrogen presents itself to the heat transfer investigator as an ideal fluid for the investigation of some unusual regimes of heat transport.

One of these can be classified as the two-phase region (subcritical temperature, subcritical pressure). For this entire regime, the bulk temperature is never more than 30^{o} below the critical temperature.

Also because of the extremely low bulk temperature (circa 40° to 50° R) the driving temperature from wall to bulk may be of the order of 1000° to 1500° F without exceeding a tolerable wall temperature. Consequently, convective boiling heat transfer far into the film boiling condition can be reproduced. The second region is one where pressure is somewhat above critical pressure (188 to 800 psia) and the temperature is from 45° to 150° R. A third region involves very high pressures (greater than 800 psia) and low bulk temperatures. Very little heated-tube experimental data has been obtained in this region and thus it remains a region for future experimental exploration. A fourth region is that of temperatures above 200° R, and the pressure varying from 1 atmosphere to 100 atmospheres. In this region standard gas phase pipe flow correlations as given in reference 1 seem to apply. The fourth region is seldom encountered in nozzle cooling applications and will not be considered in detail.

Boiling heat transfer. - Correlation of the heat transfer results for film boiling hydrogen is presented in reference 4. The approach used in the correlation involves the assumption of an annular-like two-phase flow model. As is illustrated in figure 4, an annulus of vapor surrounds a core of liquid. A turbulent exchange of vapor and liquid takes place across the boundaries between the two phases. This exchange is perhaps the chief mechanism of heat transport.

The correlation approach taken was similar to some prior work done by Dengler and Addoms (ref. 14), and Guerrieri and Talty (ref. 15), for convective nucleate boiling heat transfer. They had shown that the Martinelli two-phase parameter (originally developed to correct for the

total shear in two-phase flow) was applicable as a principle parameter of correlation of the heat transfer results. The Martinelli parameter, as expressed below in equation form, is primarily dependent on the mass ratio of vapor to liquid phases.

$$X_{tt} = \left(\frac{\dot{w}_l}{\dot{w}_g}\right)^{0.9}\left(\frac{\mu_l}{\mu_g}\right)^{0.1}\left(\frac{\rho_g}{\rho_l}\right)^{0.5} \qquad (9)$$

Figure 5 presents the heated tube data from reference 4 in terms of the correlation. The parameters of the ordinate which include a ratio of the experimental Nusselt number to an estimated Nusselt number are discussed more fully in reference 4, and are defined in appendix A.

In examining figure 5, it is interesting to observe that the correlation covers a broad range of two-phase conditions. The high values of X_{tt} represent a near-liquid condition while the low values represent the near-gaseous condition. At the latter condition the correlation approaches the gaseous correlation described previously.

The pressure drop in the test section was observed to be much greater than any value predicted from the application of friction factors. It turned out the pressure drop observed was chiefly momentum change caused by rapid density changes through the test section. A simple, one-dimensional momentum change calculation was adequate for predicting the pressure drop.

Near-Critical Heat Transfer

Within this domain the pressure range is somewhat above the critical pressure and the fluid temperature is both above and below the critical value. In rocket cooling applications this domain is likely to be encountered.

Because this region is so proximate to the critical point, the drastic gradients in fluid properties lead to difficulties in heat transfer correlations. This peculiar region has been of interest for some time for a variety of fluids including water, CO_2, N_2 and O_2, as well as hydrogen. Considerable difficulty has been incurred in correlating all of these data. Early in the hydrogen test program at the Lewis Research Center, it was evident that the data for this fluid region could not be correlated by gaseous pipe flow correlations such as are presented in references 1, 2, and 16. It was also apparent that some of the experimental results looked strikingly like the two-phase results that had been completed earlier. In particular, the axial distribution of the wall temperature for the near-critical state looked similar to that of the two-phase condition. For both situations, the wall temperature tended to peak near the entrance and then to decline in the downstream portion of the tube. This is a notably different behavior of wall temperature as observed with single phase fluids, either gases or liquids.

Some other experimental evidences of similarity between the near-critical and the two-phase heat transfer mechanisms are similarities in the wall vibrations of heat transmission as detected by sensitive pickups on the tube and similar pressure drop gradients within the tube.

On these bits of evidence and noting that earlier investigators of near-critical heat transfer (refs. 17 and 18) had postulated a boiling-like mechanism for near-critical heat transfer, a correlation approach was followed which was similar to the two-phase film boiling model. This approach is more adequately discussed in reference 5.

If it is assumed that a boiling-like mechanism is present, this presumes that a vapor or gas is being generated in the heat transfer process. Perhaps this is difficult to visualize in a fluid at supercritical pressures where there are no phase boundaries. However, it is accepted that a supercritical fluid comprises a conglomerate of molecular clusters of varying densities (ref. 19). Thus, a boiling-like mechanism can be supposed in which heat transposes heavy molecular clusters into light molecular clusters that are similar to gases. Essentially the model of the heat transport mechanism assumed is identical to that of the subcritical film boiling (fig. 4). A thin annulus of a light density gas is generated adjacent to the wall and a turbulent exchange exists between this annulus and a core of heavier fluid. This is a very simplified picture of the process. Probably a more realistic picture would consider a complex distribution of molecular clusters of varying density. However, there is no tractable method for prescribing such a distribution of species, so an approximate description is needed. The first approach that was made at the Lewis Research Center was to consider the fluid to be made up of two-density species - a heavy and a light species. A perfect gas density was assigned as the light species and the melt density as the heavy species. The latter was considered to represent the perfect liquid structure. Mixture of these two species in appropriate mass fractions produced the local bulk density obtained from measurements.

$$\frac{1}{\rho_b} = \frac{x_2}{\rho_{pg}} + \frac{1 - x_2}{\rho_{melt}} \tag{10}$$

From the above equation the pseudo quality x_2 can be computed readily. Knowing the local pseudo quality, the correlation scheme followed closely

the method utilized with the two-phase convective film boiling of hydrogen. Again the Martinelli two-phase parameter was used as a principle parameter of correlation. The other parametric grouping was a ratio of experimental to computed Nusselt numbers which resembled the two-phase grouping. Film properties were used to compute these Nusselt numbers. The equations and designation of properties are tabulated in appendix A. The reader can readily compare the two-phase (subcritical pressure) with the pseudo two-phase (supercritical pressure) calculations in this appendix.

Looking at figure 6, it is apparent that this manner of correlating the near-critical data does provide a fairly accurate correlation and one which is surprisingly similar to the subcritical correlation (fig. 5). Both the subcritical and the supercritical correlations are presented and compared in reference 5.

Recently, some modifications to the supercritical correlation have been incorporated but have not yet been reported in the literature. Principle in these modifications have been a redefinition of the heavy density in the pseudo-two-phase definition, and the introduction of another dimensionless grouping in the overall correlation. This grouping which has been called a discharge ratio is similar to Sterman's parameter (ref. 20) for two-phase convective heat transfer. For the real two-phase situation, this parameter can be looked upon as a ratio of how much heat is absorbed by the latent heat to how much is absorbed by sensible heating for a flow of fluid through a heated channel. For a fluid near its critical point the latent heat can be considered to be equivalent to the discontinuous

or rapid change in specific heat. Such a change can be expressed in terms of an enthalpy change.

These modifications to the original correlation that appeared in reference 5 have improved the applicability of the correlation scheme over a broader range of experimental conditions. However, as noted in reference 5 the applicability of the pseudo two-phase approach is limited to pressures of about 800 psia and compressibility factors of unity or less.

High pressure heat transfer. - Experimental data for heat transfer to hydrogen at pressures above 800 psia and temperatures below 150° R is extremely limited. Thompson and Geery present data for this region in reference 3 and they also present a correlation which can be used. The correlations of references 1 and 2 are probably also applicable for the high pressure, low temperature regime because the variations of properties at high pressures is much less severe than for the lower pressures.

DESIGN PROCEDURE

To study the design procedure, a tubular regeneratively cooled nozzle will be considered. The design of such a hydrogen regenerative cooling system is an iteration process. This iteration involves both the coolant tube stresses and the coolant pressure drop as well as the heat transfer considerations. As a start, the wall temperature at each axial station, the coolant inlet pressure, and tube wall thickness can be assigned, and the number of tubes and tube material selected on the basis of tube wall stresses.

The steps in the heat transfer calculations are:

a. Evaluate the heat flux into the nozzle wall from nozzle geometry and propellant gas flow and transport properties.

b. Compute the coolant side wall temperature from heat flux, wall thickness, and wall material thermal conductivity.

c. Determine coolant tube diameter from heat flux, inner wall temperature, coolant temperature and transport properties.

d. Evaluate coolant pressure drop.

It should be noted that steps c and d are integration processes in that coolant temperature, pressure, and transport properties are dependent on conditions at preceding stations along the coolant flow path. Care must be exercised to avoid choking of coolant channels. When overall pressure drop has been determined, the pressure drops between the coolant tube outlet and the rocket chamber can be evaluated. If the resultant chamber pressure is different than desired, a new coolant system inlet pressure is assigned and the process repeated. If choking of the coolant tubes is encountered or if the calculated overall pressure drop is excessive, the initial assumptions regarding tube material, the limiting temperature or number of tubes must be changed and the process repeated. When a design has been obtained that is satisfactory in regards to pressure drop and coolant passage discharge pressure, the tube material stresses must be checked.

Hot gas side heat flux. - Three potential methods of evaluating the gas side heat transfer coefficient have been discussed. The boundary layer technique is considered to be the most basic approach. The pipe flow type approaches can be used if appropriate values of the constant C (eq. (2)) are known.

For chemical systems, the combustion inefficiency should be considered in the evaluation of gas enthalpy. Gas temperature has been

corrected on a basis of the combustion efficiency squared. When the enthalpy difference is considered as driving potential, a correction must be made for both the recovery and wall enthalpy of the gas. These two corrections may compensate for one another. The biggest question in applying these correlations to a nozzle composed of a tube bundle lies in the irregular circumferential contour of this type of nozzle. This contour is illustrated in figure 7. The figure shows a longitudinal cross section normal to the nozzle axis. In general, the inner surface of the tubes are essentially semicircular. Each tube is flattened slightly on the sides to facilitate brazing or welding, and the whole bundle is wire-wrapped or contained by some type of pressure shell. As illustrated, the inner circumferential profile is made up of a series of semicircular tubes joined by braze or weld fillets. The hot gas side heat transfer calculations, however, are based on a circular inner cross section.

The standard assumption made in current design approaches is to assume the available techniques of computing heat flux will apply for a region near the center of the portion of the tube which is exposed to the hot gas (point A of fig. 7). In the region between tubes the fin effect of the sides of the tube will increase the coolant effectiveness. The fillet region (point B on fig. 7) should therefore, be cooler than the center portion of the coolant tube. If the cooling is adequate to maintain a safe temperature at the center (point A), the tube will not burn out.

The anticipated temperature distribution and heat flux variation across the face of an individual tube has been calculated using a relaxation technique. Variation of hot gas side heat transfer coefficients

were estimated from theoretical calculations by Deissler (ref. 21) for a rectangular array of tubes. The coolant side heat transfer coefficient was assumed constant around the tube circumference. This assumption will be discussed in more detail later. These calculations indicate that the temperature at the center of the inner surface of the tube (point A) was 1968° R. This is very close to that computed by the assumption of a circular inner surface. The calculated temperature at the fillet point B however, was only 545° R. Total heat flux into the coolant at any axial station must be obtained by an integration of local heat flux around the tube. For this particular case, the integrated heat flux was 1.25 times that computed for the pure circular inner surface shape by conventional techniques. This difference in heat flux into the wall surface indicates that the larger surface area and the higher driving potential between the hot gas and the wall in the fillet region more than offset the lower heat transfer coefficient in the fillet region.

These calculations are at best approximations, and more detailed data of wall temperatures and heat flux variations are required for complete answers. Lacking better information on the tube shape and fin effect, a method of computation based on a circular cross section must be used. It appears that this approach is satisfactory in determining maximum wall temperature. Some correction for nonuniform heating should be made in calculating the heat rejection to the coolant. For chemical rockets the injector design has been shown to have a marked effect on gas side heat transfer coefficients (ref. 13). In general, efficient injectors will give maximum heat fluxes.

Wall conduction calculations. - In order to determine the coolant side, wall temperature, the temperature drop across the wall must be considered. As shown in reference 22, the temperature drop across the wall can be appreciable if high heat fluxes, such as those estimated for nuclear rocket nozzle, are encountered. The temperature drop across the wall could be computed by a complex relaxation method such as discussed above. For most cases, however, a simple conduction calculation which neglects circumferential conduction is adequate insofar as maximum local tube wall temperature is concerned.

Coolant side heat flux. - For the coolant side calculations, the procedure is to evaluate the coolant tube cross sectional area required to absorb the heat flux rejected to the wall by the hot gas. The width of the tube is set by the local nozzle diameter, the number of tubes and the tube wall thickness. Thus, the tube geometry is generally defined in terms of the tube height. The appropriate correlation for subcritical or supercritical pressure must be used. As for the hot gas side, the coolant calculation is applied at the center of the tube surface which is exposed to the hot gas.

Several simplifying assumptions are involved in this approach. The correlations discussed previously are for straight, constant diameter tubes with constant heat flux both circumferentially and axially. The correlations are for center portions of test sections where entrance effects are neglected. In the rocket coolant tube, the heat flux varies both axially and circumferentially; the tube diameter varies along the tube length, and near the throat the tube may have rather large curvatures. In addition,

near the entrance of the coolant tube, the region of development of viscous and thermal boundary layers may seriously alter the heat flux.

Barrow (ref. 23) has studied the heat transfer between parallel plates with unequal heat addition. His studies indicate a reduction in heat transfer coefficient over that for uniform heat input. This would indicate that nonuniform heating of the nozzle coolant tube would result in a reduction of heat flux from that predicted by available data. Limited unpublished data for heated tubes has verified this fact, but has also shown the magnitude of reduction to be of the order of 15 percent.

Some preliminary data on the effects of large axial gradients of heat flux have been obtained at the Lewis Research Center. These tests indicate small increases in heat transfer coefficient for the case of increasing heat flux in the flow direction, and slight decreases for the decreasing case. A similar observation is presented in reference 24 which involves an analysis of a turbulent boundary layer across a flat plate. One may surmise that curvature effects near the throat of conventional convergent-divergent nozzles may be favorable due to boundary layer secondary flows. At the entrance to the convergent section, however, these effects would be reversed. No conclusive data are available on effects of tube curvature. Entrance effects will be favorable in regards to heat transfer, although they may lead to underestimates of coolant bulk temperatures. Inasmuch as coolant heat transfer is primarily a function of specific mass flow, neglecting entrance effects will not be serious in nozzle design unless the coolant passage is designed close to the choking flow condition. However, some errors in coolant outlet temperature and pressure may result.

All of these problem areas represent pertinent research areas and may prove to be severe design limitations where cooling is marginal. For most conservative design, however, the use of the hydrogen heat transfer correlations presented should lead to acceptable designs.

In addition to the heat flux calculations the pressure drop in the coolant tube must be calculated. Many of the questions which arise in the calculation of heat flux also affect the pressure drop. The use of standard friction factors and momentum pressure loss estimates will, however, generally be satisfactory.

Sample design. - The calculation of the hot gas side heat transfer is a straightforward noniterative calculation. Coolant side calculations, on the other hand, must be done stepwise along the coolant tube in order to accurately evaluate the coolant pressure level. If calculations are made at sufficiently small intervals, the rate of pressure loss from one station can be extrapolated to evaluate the coolant pressure at the succeeding station. For wider spacing of stations, an average pressure drop rate should be used. This process involves an iteration procedure.

Figure 8 presents the wall temperature distribution and heat flux along the axial length of a representative nozzle for a hydrogen-oxygen rocket. The nozzle contour is also shown in this figure. Because the coolant flow enters at the nozzle exit and flows towards the injector, the nozzle exit is shown in the left of this figure. The wall temperature is a maximum at the throat and decreases at the injector face and nozzle exit. Heat flux is also a maximum at the nozzle throat.

The variations in coolant passage height, bulk temperature, and coolant pressure are shown in figure 9. This particular design is for

nuclear rocket simulation. Therefore, the coolant flow is higher and the bulk temperature rise is less than expected for a conventional hydrogen, oxygen rocket cooling system. The bulk temperature increases almost linearly from the entrance to the exit. This indicates that the maximum heat flux per unit area in the vicinity of the throat is offset by the smaller heat transfer area in this region. Coolant passage height decreases from the nozzle exit to the throat and then increases sharply. Because of the change in passage width, the coolant passage flow area variation is even more extreme than the passage height shown on figure 9. The major portion of the coolant pressure drop occurs near the throat of the nozzle.

SUMMARY REMARKS

The design of a hydrogen convectionally cooled rocket nozzle is an iteration process between material stresses, heat flux, and pressure drop. Calculation for a nozzle design requires a knowledge of hot gas side heat flux, wall conduction processes, and coolant side heat transfer. On the hot gas side, the major problem relates to the convergent region of the nozzle. For the divergent region, the Nusselt type correlation based on a three-dimensional $\rho_s V_s$ value or the boundary layer approaches can be used to predict heat flux. On the basis of data presented herein the boundary layer approach is more basic and somewhat more accurate, but the Nusselt type correlation is simpler to apply. For the convergent region of the nozzle, both approaches are open to question. The variation of the coefficient in the Nusselt correlation must be known for the particular nozzle geometry. Selection of the initial upstream conditions for the boundary layer solution presents a similar problem. Effects of injection process on heat flux in the convergent region also results in

appreciable variations in heat flux. On the coolant side, hydrogen presents some peculiarities due to the fact that the coolant will be at subcritical temperatures and either sub or supercritical pressures throughout a portion of the nozzle. Correlations for uniform circumferential and axial heat flux are available. More research, however, is needed on effects of nonuniform heat flux, tube curvature effects and tube entrance effects. Further research for pressures above 800 psia is also desirable.

For conservative designs the available data and approaches are adequate. For those designs where cooling is marginal or pressure drops appreciable, development may be required to obtain a reliable cooling system.

APPENDIX A

For both the film boiling and near-critical heat transfer of hydrogen similar correlation techniques were applied. As was discussed in the main body of the paper, the model of heat transport is substantially the same for both of these fluid states. Figure 4 depicts this model concept. The pertinent definitions and equations that relate to the correlations are outlined below. They will be presented for both of the fluid states, so that they can be compared.

Boiling		Near-critical	
(a) Quality (mass fraction of light species)			
$\frac{1}{\rho_b} = \frac{x}{\rho_{pg,b}} + \frac{1-x}{\rho_l}$	(1a)	$\frac{1}{\rho_b} = \frac{x_2}{\rho_{pg,b}} + \frac{1-x_2}{\rho_{melt}}$	(1b)
(b) Calculated Nusselt number (ordinate of figs. 5 and 6)			
$Nu_{calc} = 0.023 \left(\frac{\rho_{fm} V_{av}\, d}{\mu_f}\right)^{0.8} (Pr)^{0.4}$	(2a)	$Nu_{calc} = 0.023 \left(\frac{\rho'_{fm} V_{av}\, d}{\mu_f}\right)^{0.8} (Pr)^{0.4}$	(2b)
where the densities are defined as			
$\frac{1}{\rho_{fm}} = \frac{x}{\rho_{pg,f}} + \frac{1-x}{\rho_l}$	(3a)	$\frac{1}{\rho'_{fm}} = \frac{x_2}{\rho_{pg,f}} + \frac{1-x_2}{\rho_{melt}}$	(3b)
(c) The Martinelli parameter			
$\chi_{tt} = \left(\frac{1-x}{x}\right)^{0.9} \left(\frac{\mu_l}{\mu_{pg}}\right)^{0.1} \left(\frac{\rho_{pg}}{\rho_l}\right)^{0.5}$	(4a)	$\chi'_{tt} = \left(\frac{1-x_2}{x_2}\right)^{0.9} \left(\frac{\mu_{melt}}{\mu_{pg,f}}\right)^{0.1} \left(\frac{\rho_{pg}}{\rho_{melt}}\right)^{0.4}$	(4b)

REFERENCES

1. McCarthy, J. R., and Wolf, H.: "Forced Convection Heat Transfer to Gaseous Hydrogen at High Heat Flux and High Pressure in a Smooth Round, Electrically Heated Tube." ARS Journal, April 1960, p. 423.

2. Wright, C. C., and Walters, H. H.: "Single Tube Heat Transfer Tests of Gaseous and Liquid Hydrogen." WADC Tech. Report 59-423.

3. Thompson, R. W., and Geery, E. L.: "Heat Transfer to Cryogenic Hydrogenic at Supercritical Pressures," Aerojet Report 1842, Aerojet General Corp., July 1960.

4. Hendricks, R. C., Graham, R. W., Hsu, Y. Y., and Friedman, R.: "Experimental Heat Transfer and Pressure Drop of Liquid Hydrogen Flowing Through a Heated Tube." NASA TN D-765, May 1961.

5. Hendricks, R. C., Graham, R. W., Hsu, Y. Y., and Medeiros, A. A.: "Correlation of Hydrogen Heat Transfer in Boiling and Supercritical Pressure States." ARS Journal Feb. 1962, p. 244.

6. Eckert, E. R. G., and Drake, R. M., Jr.: Heat and Mass Transfer. McGraw-Hill Book Co., Inc., 1959.

7. Brokaw, R. J.: Planetary Space Science, 3, 1961, p. 238.

8. Bartz, D. R.: A Simple Equation for Rapid Estimation of Rocket Nozzle Convective Heat Transfer Coefficients. Jet Propulsion, Jan. 1957, pp. 49 to 51.

9. Reshotko, Eli, and Tucker, Maurice: Approximate Calculation of the Compressible Turbulent Boundary Layer with Heat Transfer and Arbitrary Pressure Gradients. NACA TN-4154, Dec. 1957.

10. Cohen, N. B.: A Method for Computing Turbulent Heat Transfer in the Presence of a Streamwise Pressure Gradient for Bodies in High Speed Flow. NASA Memo. 1-2-59L, March 1959.

11. Bartz, D. M.: An Approximate Solution of Compressible Turbulent Boundary-Layer Development and Convective Heat Transfer in Convergent, Divergent Nozzles. Transactions of the ASME, Nov. 1955, pp. 1235-1245.

12. Rao, G. V. R.: Exhaust Nozzle Contours for Optimum Thrust Jet Propulsion. Vol. 28, no. 6, June, 1958.

13. Welsh, W. E., Jr., and Witte, A. B.: A Comparison of Analytical and Experimental Local Heat Fluxes in Liquid-Propellant Rocket Thrust Chambers. Technical Report 32-43, Jet Propulsion Laboratory, Feb. 1, 1961.

14. Dengler, C. E., and Addoms, J. N.: Heat Transfer Mechanism for Mechanism for Vaporization of Water in a Vertical Tube. Heat Trans. Symposium, Louisville. Vol. 52, no. 18, 1956, p. 95.

15. Guerrieri, S. A., and Talty, R. D.: A Study of Heat Transfer to Organic Liquids in Singe-Tube Natural Circulation Vertical Tube Boilers. Heat Trans. Sym., Louisville. Vol. 52, no. 18, 1956, p. 69.

16. Taylor, M. F., and Kirchgessner, T. A.: Measurement of Heat Transfer and Friction Coefficients for Helium Flowing in a Tube at Surface Temperatures up to 5900° F. NASA TN D-133, 1959.

17. Goldmann, K.: Special Heat Transfer Phenomena for Supercritical Fluids. Nuclear Develop. Corp. Report 2-31, Nov. 1956.

18. Dickinson, N. L., and Welch, C. P.: Heat Transfer to Supercritical Water. ASME Paper 57-HT-7.

19. Frenkel, J.: Kinetic Theory of Liquids. Dover Publications, Ch. 7, New York, 1946.

20. Sterman, L. S.: On the Theory of the Heat Transfer from a Boiling Fluid. Zhurnal Tekhnicheskoi Fiziki 23 (2) 341-351, 1953.

21. Deissler, R. G., and Taylor, M. F.: Analysis of Turbulent Flow and Heat Transfer in Non-Circular Passages. NASA TR-R-31, 1959.

22. Robbins, W. A., Backin, D., and Medeiros, A. A.: An Analysis of Nuclear Rocket Cooling. NASA TN-D-482, 1960.

23. Barrow, Henry: Convection Heat Transfer Coefficients for Turbulent Flow Between Parallel Plates with Unequal Heat Fluxes. International Journal of Heat and Mass Transfer I, (1961), 306-311.

24. Reynolds, W. C., Kays, W. M., and Kline, S. J.: Heat Transfer in the Turbulent Incompressible Boundary Layer. NASA Memo 12-3-58-W.

TABLE I

$\frac{l}{d_t}$	$h_{i,ex}$, lb/(sec)(sq in.)	$\frac{h_{i,ex}}{h_{i,BL}}$, Case 1	$\frac{h_{i,ex}}{h_{i,BL}}$, Case 2	$\frac{h_{ex}}{h_{N-3D}}$	$\frac{h_{ex}}{h_{N-1D}}$
-1.9	0.197×10^{-2}	1.43	1.82	1.76	1.76
-.5	.463	.910	1.03	.99	.99
-.34	.640	1.00	1.13	1.10	1.10
-.17	.643	.90	1.01	.99	.99
+.05	.514	.78	.87	1.00	.82
+.09	.451	.75	.84	.97	.74
+.185	.349	.77	.87	1.05	.66
+.33	.295	.76	.85	1.03	.75
+.94	.188	.81	.89	1.11	1.17
+1.56	.133	.85	.94	1.18	1.47
+2.17	.107	.92	1.01	1.27	1.75
+2.81	.086	.95	1.03	1.30	1.88
+3.41	.072	.96	1.04	1.30	1.93
+4.02	.056	.88	.95	1.19	1.79
+4.64	.047	.88	.94	1.18	1.77
+5.26	.043	.91	.97	1.21	1.82
+5.88	.037	.88	.94	1.16	1.74
+6.49	.031	.83	.88	1.08	1.61
+6.98	.033	.96	1.02	1.25	1.84

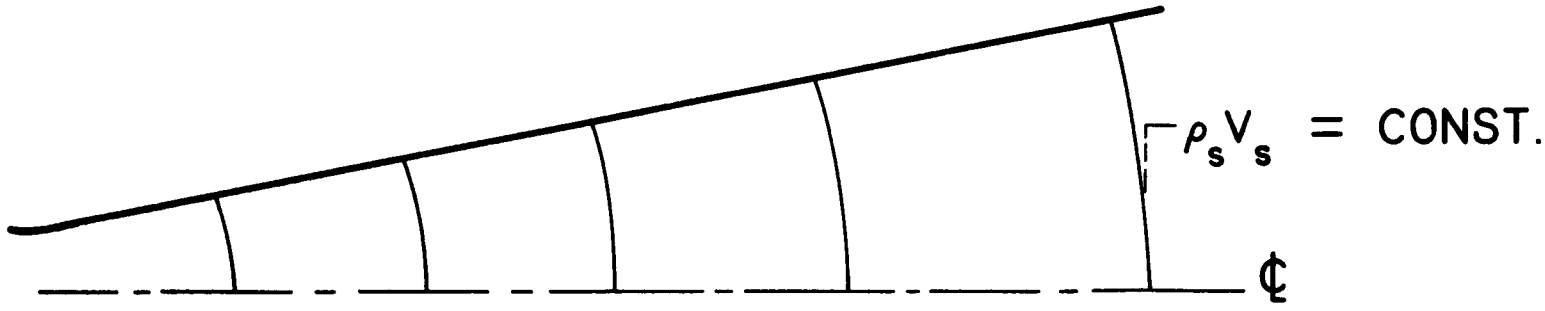

(a) Conical nozzle.

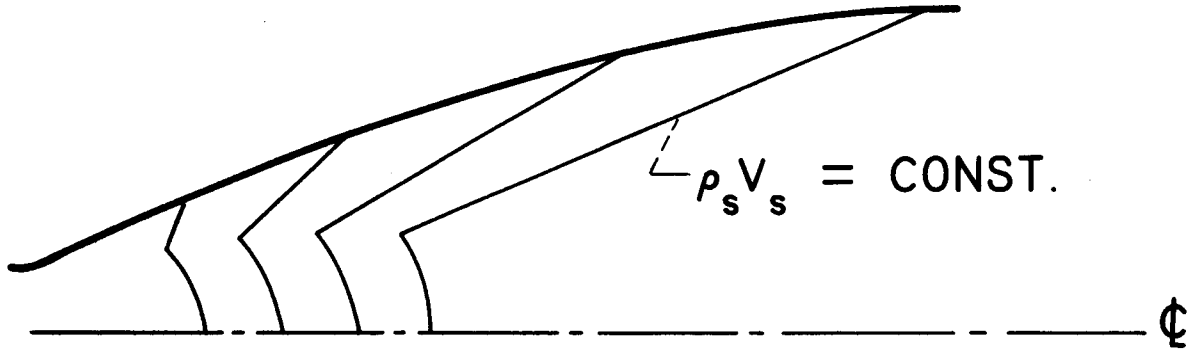

(b) Bell nozzle.

Fig. 1. - Surfaces of constant $\rho_s V_s$ for typical conical and bell nozzles.

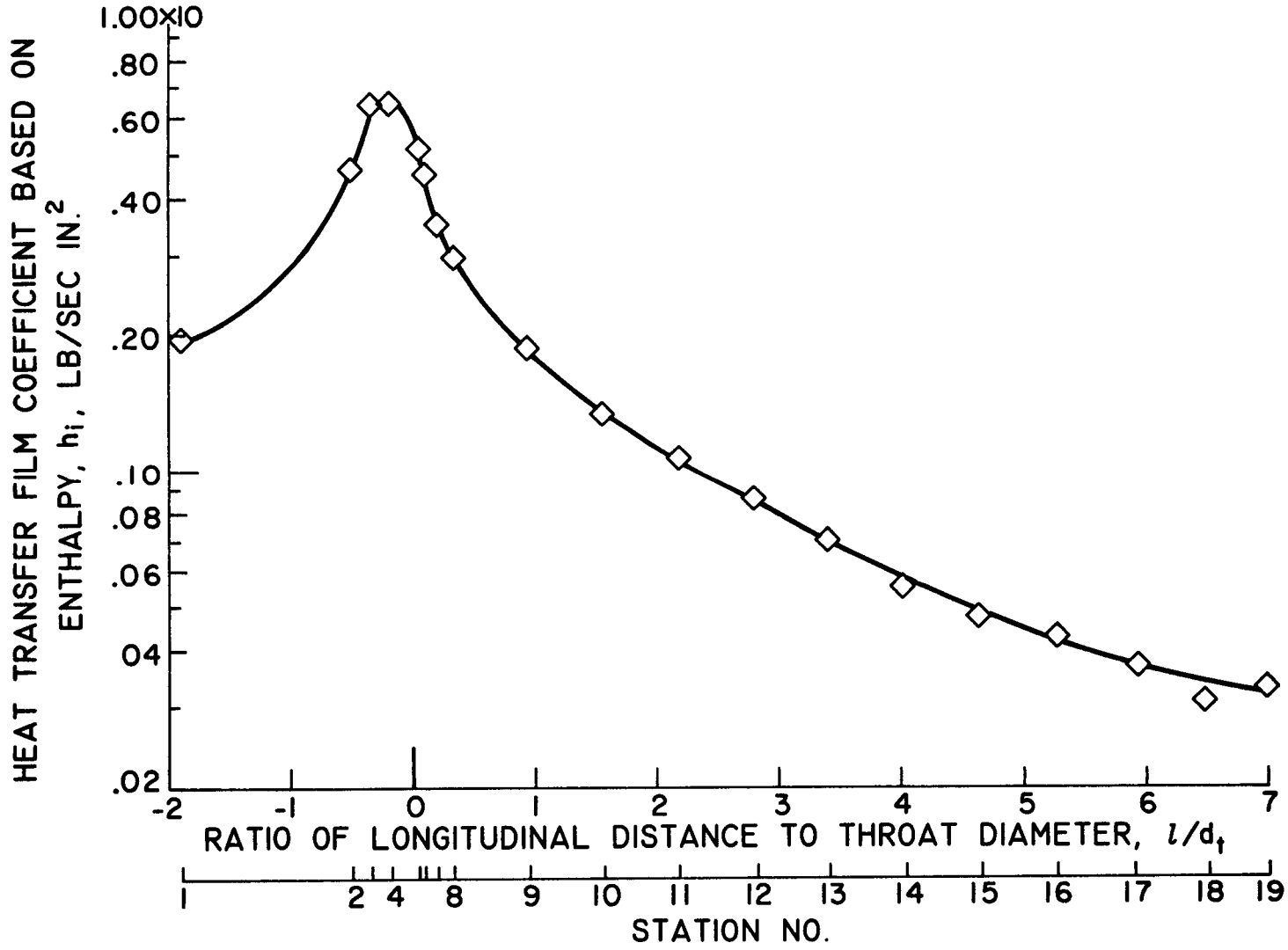

Fig. 2. - Experimental heat-transfer film coefficient in a Rao nozzle using air.

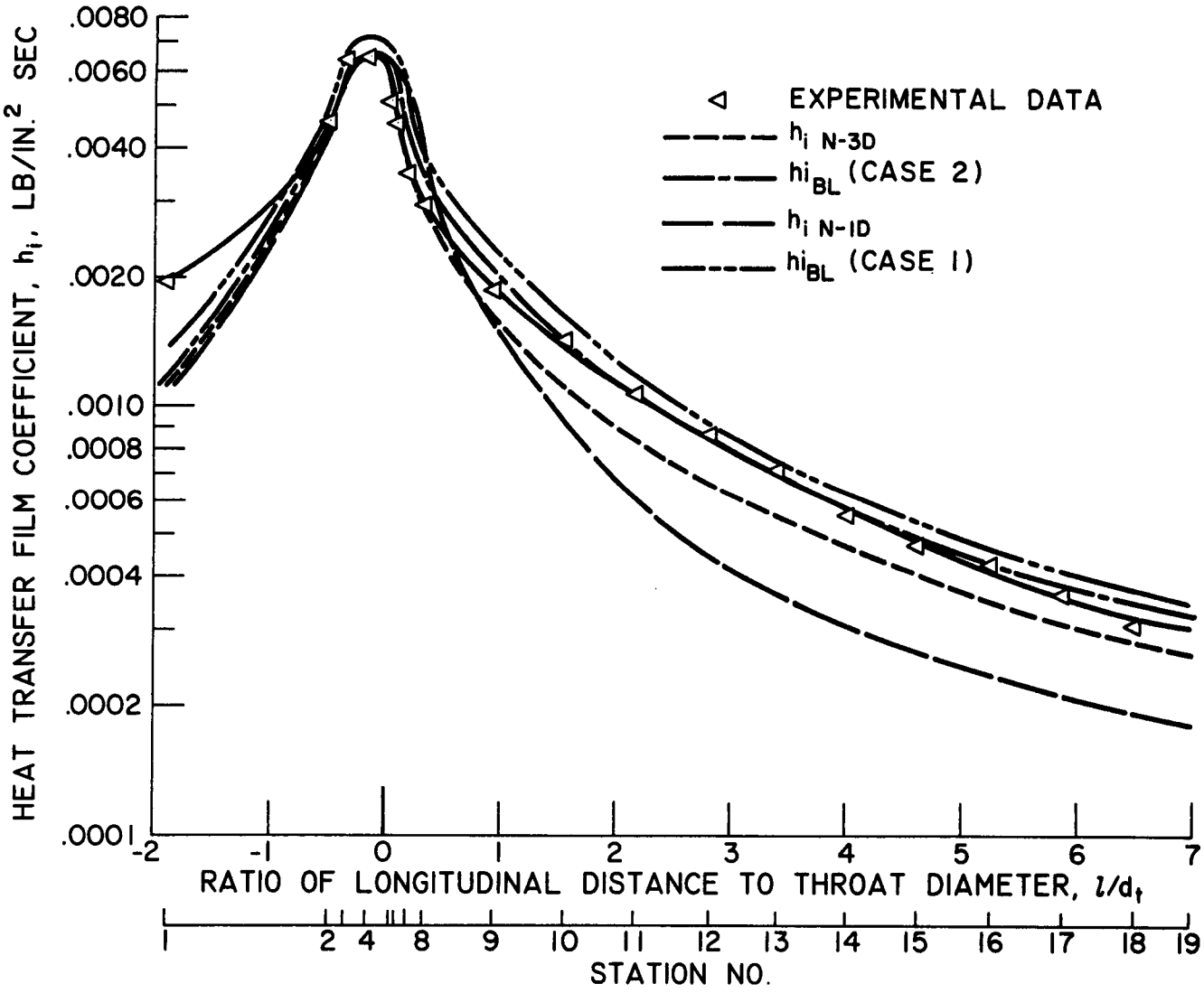

Fig. 3. - Comparison of experimental and calculated heat transfer coefficients for a bell nozzle.

E-1647

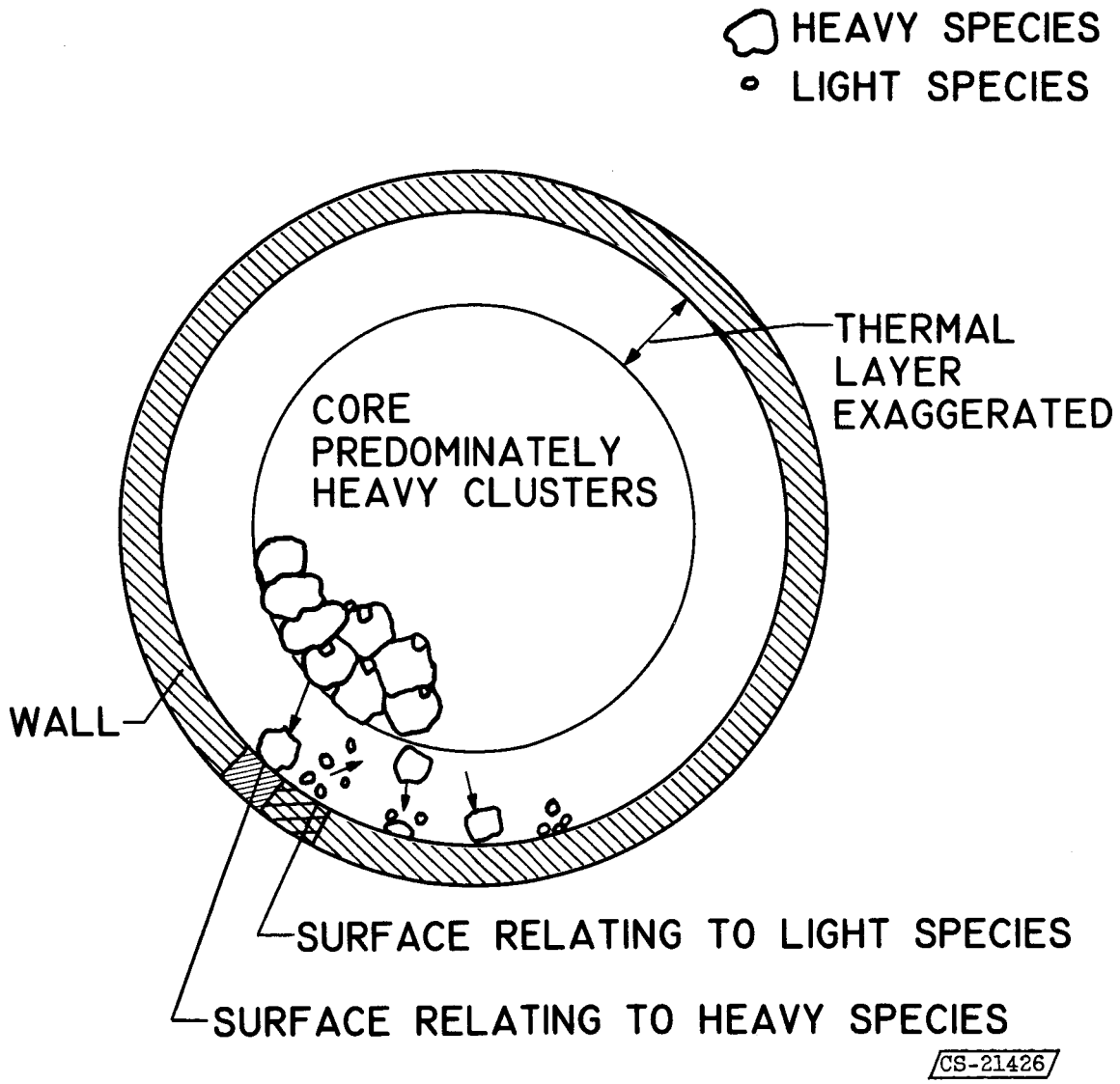

Fig. 4. - Schematic of fluid model relating to two-species heat transfer model.

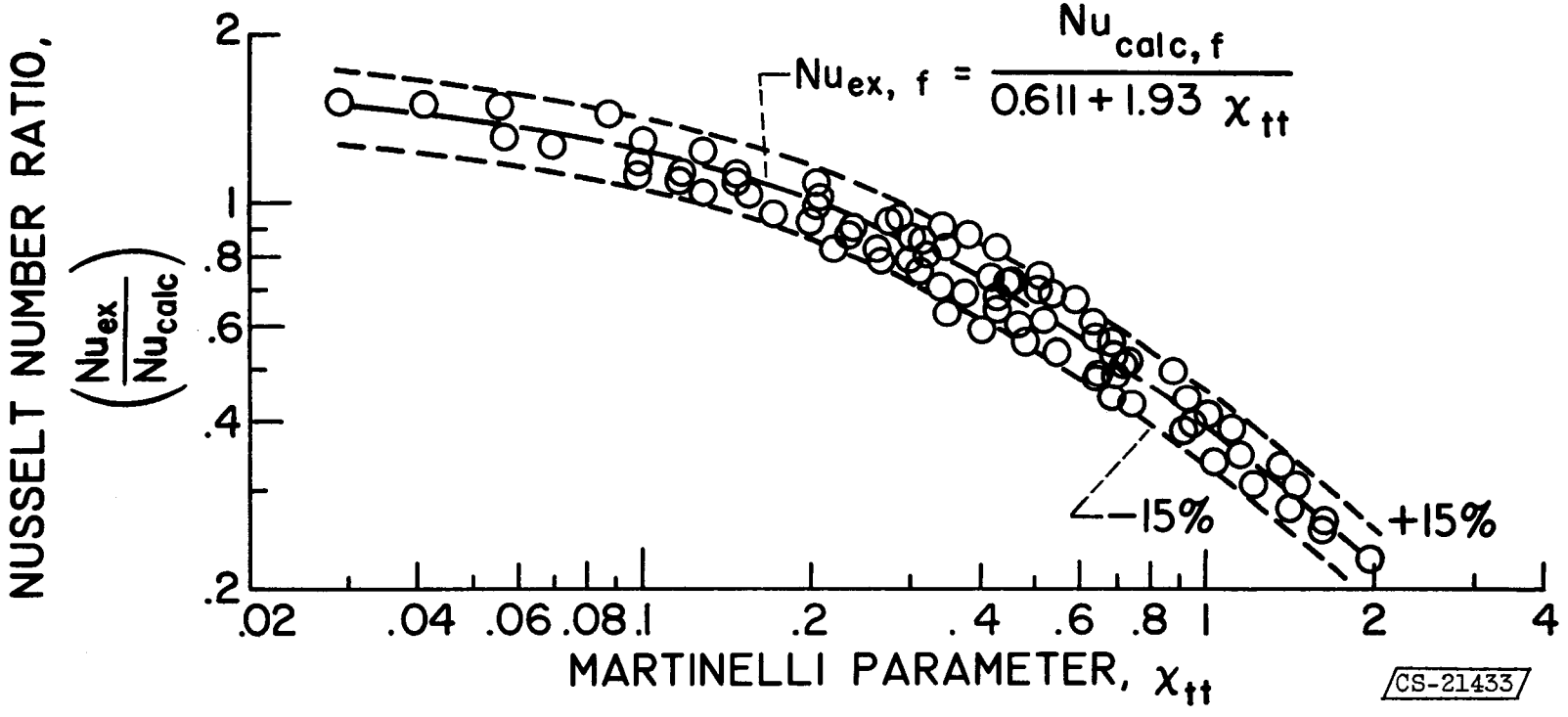

Fig. 5. - Correlation of boiling heat-transfer results with Martinelli parameter. Predicted Nusselt number based upon film conditions and corrected for quality; correlation based on data from L = 5.86 to 9.4 inches.

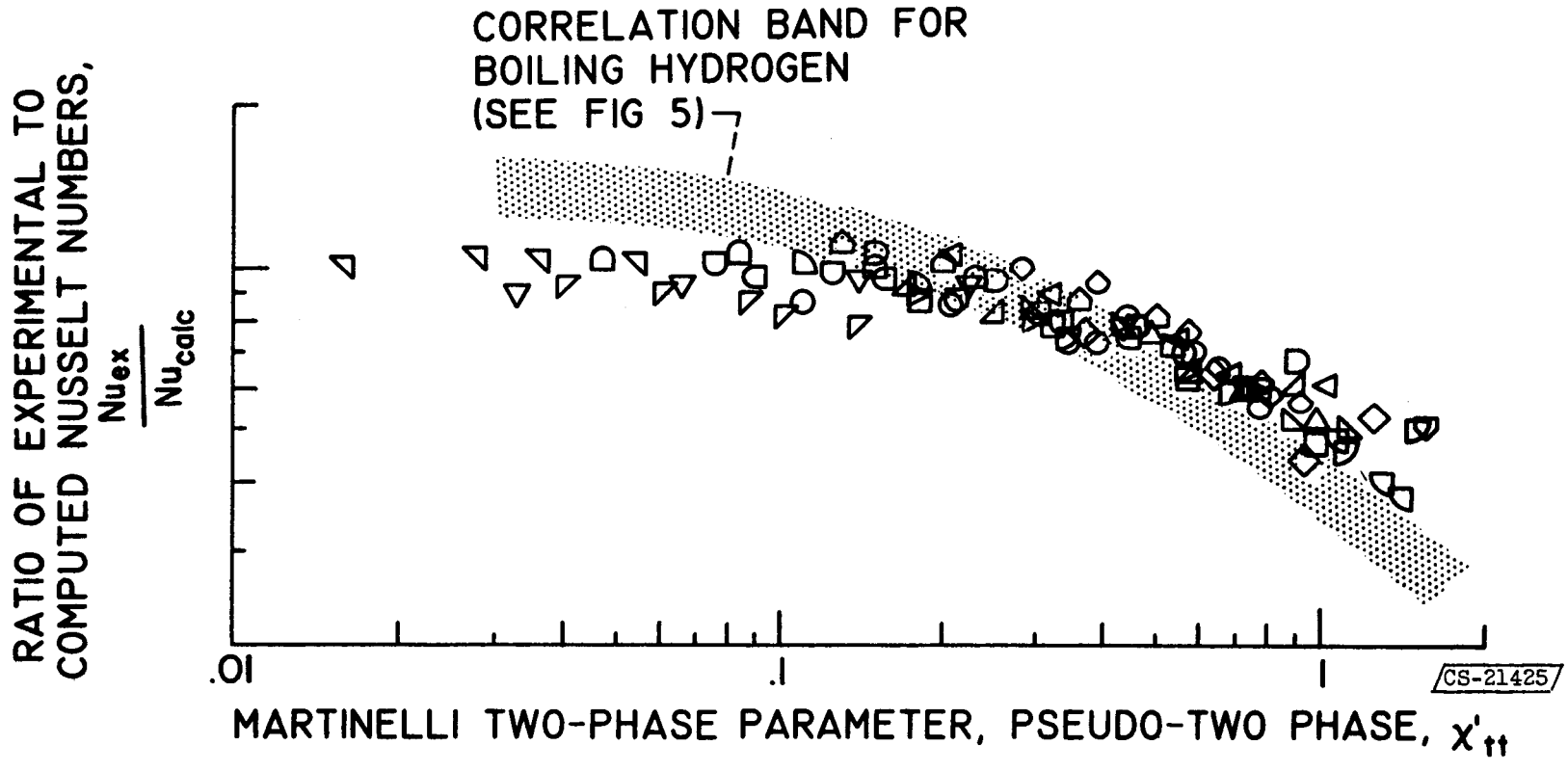

Fig. 6. - Correlation of near critical heat transfer data using modified Martinelli parameter.

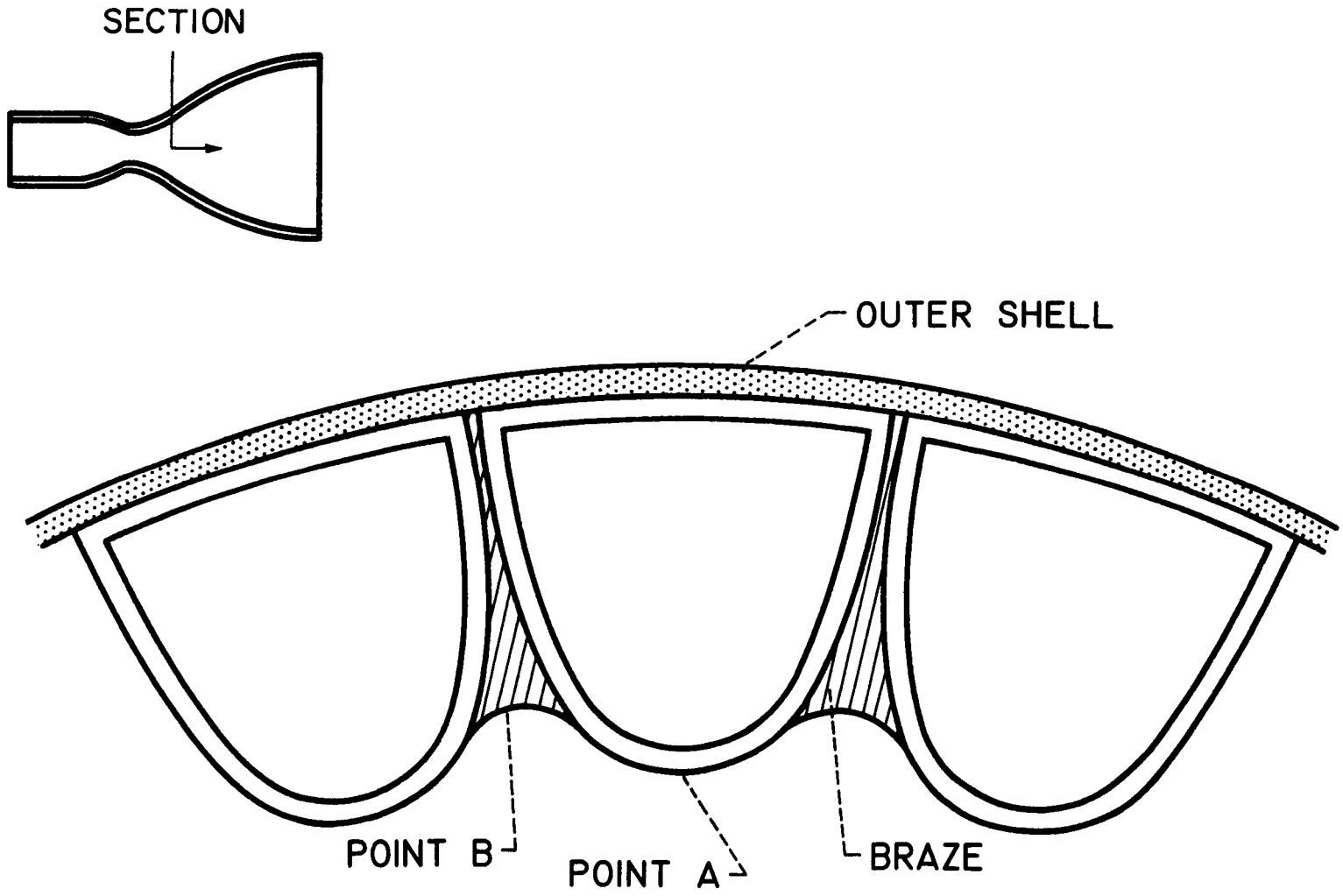

Fig. 7. - Cross-section of typical rocket engine tube bundle.

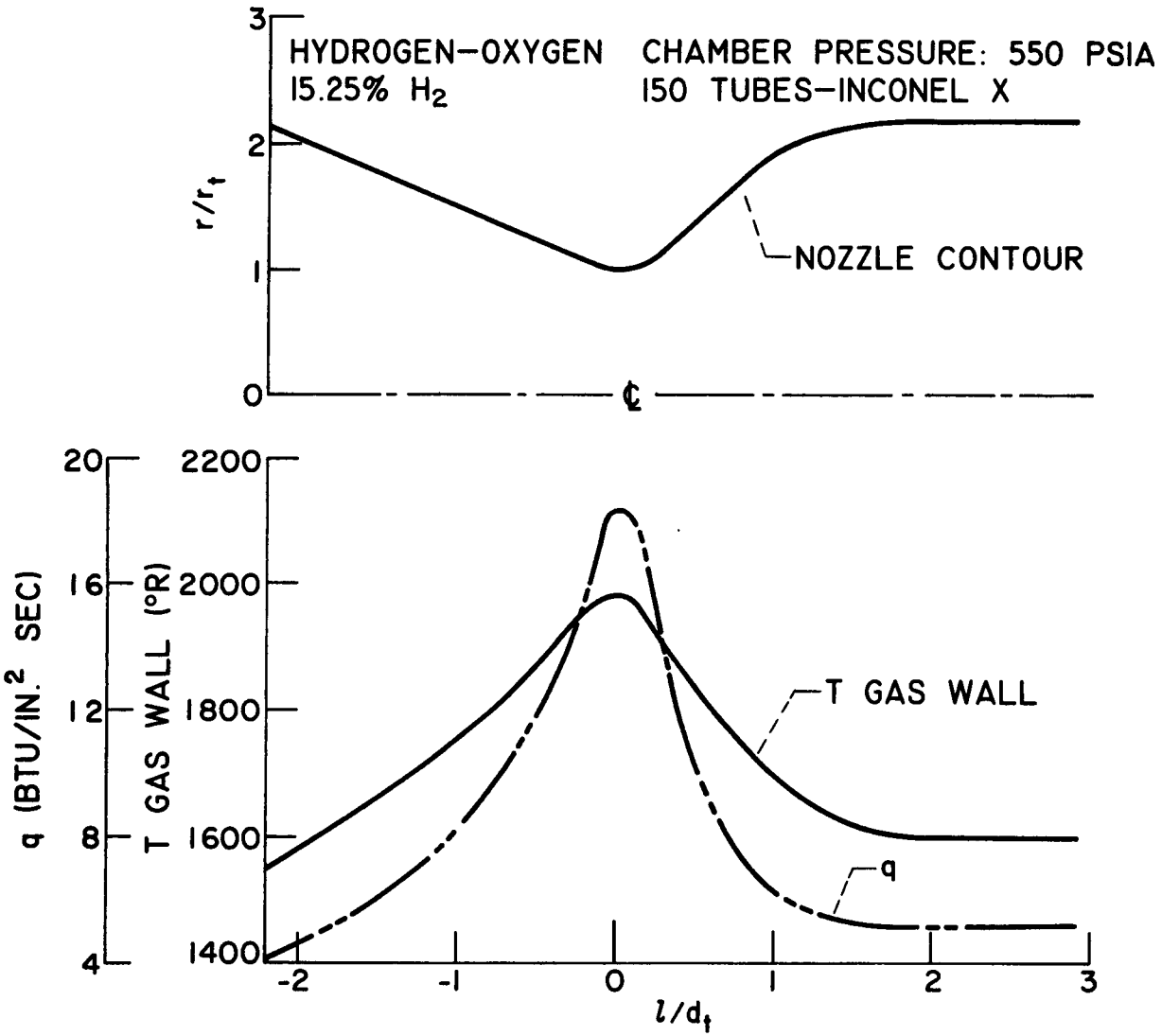

Fig. 8. - Typical nozzle wall temperature and heat flux distribution.

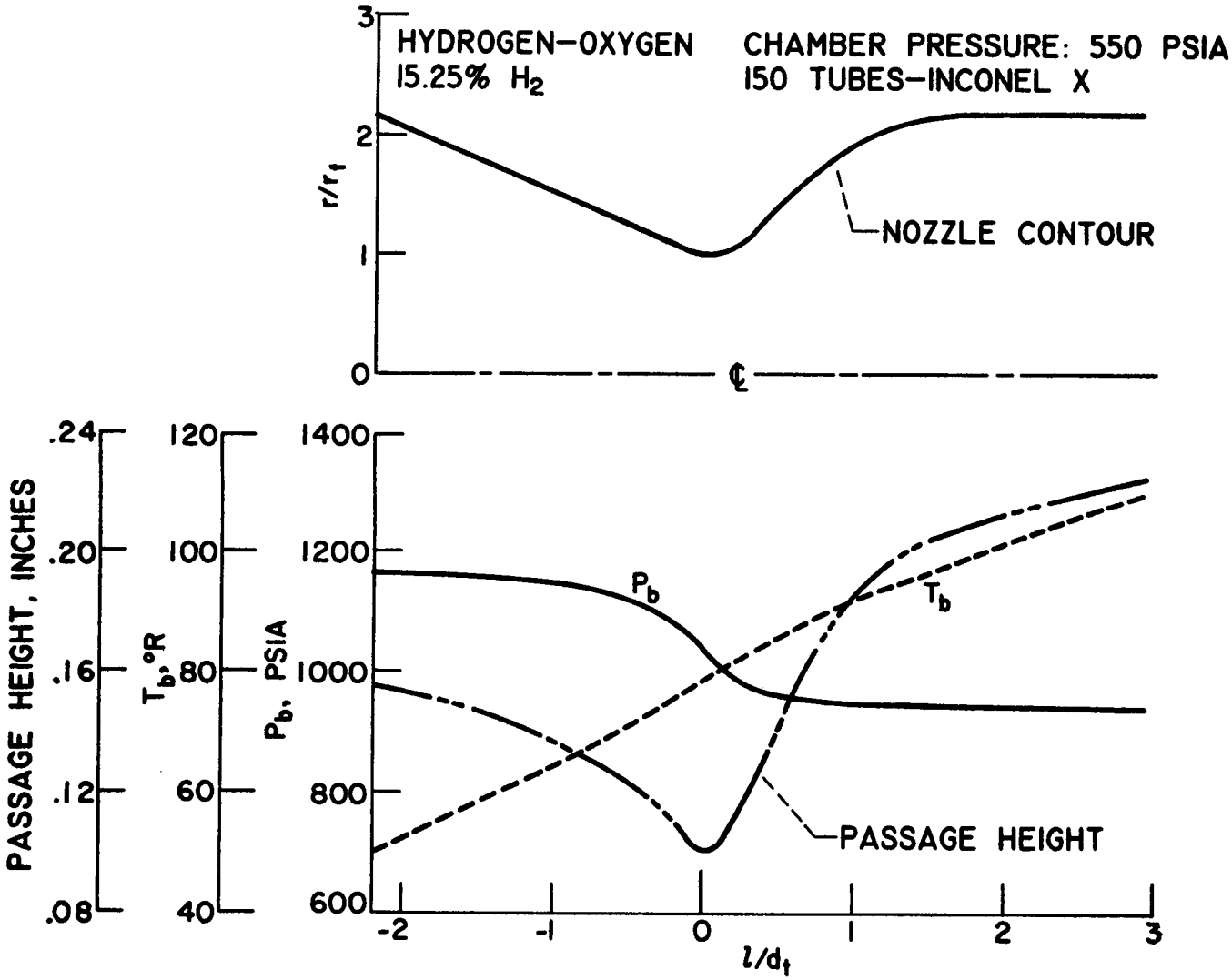

Fig. 9. - Typical nozzle coolant passage height, coolant temperature and pressure.

NASA-CLEVELAND, OHIO E-1647